IRJSE *Int. Res. J. of Science & Engineering*, 2017; Special Issue A1 : 81-86 SJIF Impact Factor 4.11
ISSN: 2322-0015 UGC Approved Journal No. 63628
**RESEARCH ARTICLE** **OPEN ACCESS**

# Selective low-temperature chlorine gas sensing properties of bio-inspired nanocrystalline $TiO_2$

**Ekar SU[1], Wani PN[2], Shaikh SF[1], Nakate UT[3], Ghule BG[1], Shinde PV[1], Raut SD[1], Jadhav VV[4], Jadhav SS[5], Khollam YB[6*] and Mane RS[1*]**

[1]Centre for Nano-materials and Energy Devices, School of Physical Sciences, Swami Ramanand Teerth Marathwada University, Nanded 431606, M.S., India.,
[2]Department of Physics, Prof. Ramkrishna More College, Akurdi, Pune 411 044, M.S., India.,
[3]School of Semiconductor and Chemical Engineering, Semiconductor Physics Research Center (SPRC) Chonbuk National University, Jeonju 54899, Jeollabuk-do, Republic of Korea (South Korea),
[4]Department of Physics, Shivaji Mahavidyalaya, Udgir 413517, M.S., India.,
[5]D. S. M. Arts, Commerce and Science College, Jintur, Parbhani 431 509, M.S., India.,
[6]Department of Physics, Baburaoji Gholap College, Sangvi, Pune 411 027, M.S., India
*Corresponding author Email: rajarammane70@gmail.com ykhollam@yahoo.co.in

**Manuscript Details**
Available online on http://www.irjse.in
ISSN: 2322-0015

**Editor: Dr. Arvind Chavhan**

**Cite this article as:**
Ekar SU, Wani PN, Shaikh SF, Nakate UT, Ghule BG, Shinde PV, Raut SD, Jadhav VV, Jadhav SS, Khollam YB and Mane RS. Selective low-temperature chlorine gas sensing properties of bio-inspired nanocrystalline $TiO_2$, *Int. Res. Journal of Science & Engineering*, December 2017; Special Issue A1 : 81-86.



**ABSTRACT**

$TiO_2$ nanoparticles (NPs) synthesized by using bio-inspired green method have shown selective low temperature gas sensing properties for $Cl_2$ gas. The $TiO_2$ NPs are characterized for their structures, morphologies, and optical studies by various means: X-ray diffraction, field emission scanning electron microscopy and UV-visible spectroscopy respectively. The average crystallite-size and band-gap of $TiO_2$ NPs are found to be respectively 7.2 nm and 3.3 eV. The $TiO_2$ NPs demonstrate good sensitivity towards chlorine ($Cl_2$) gas where $TiO_2$ NPs reveals $Cl_2$ gas response of 57 % at 250 °C operating temperature with response time of 97 s for 100 ppm concentration. The $Cl_2$ gas sensing properties are investigated for lower range 5 ppm to higher range 400 ppm. In further studies responses of $TiO_2$ as function of operating temperature and gas concentration are explored in addition to repeatability and stability measurements.

**Keywords:** Bio-synthesis, $TiO_2$, $Cl_2$ sensor, Low-temperature sensitivity, Selectivity.

## INTRODUCTION

Over the decades, semiconducting wide band-gap metal oxides are being potential materials in various areas of applications such as biomedical, water purification, solar cells, chemical and biological sensors and so on [1-6]. The semiconducting metal oxides, such as ZnO [7], $SnO_2$ [8], $WO_3$ [9], NiO [10], $TiO_2$ [11] etc., have gained attention among the solid-state sensors due to their low-costs, eco-friendly nature, availability in different dimensions, compatibility, and low-power consumption methods. The major challenges in gas sensors include fast response, low working temperature and good selectivity etc. The rapid response of sensor gives early warning or message in order to monitor the environmental gas presence. The metal oxide-based gas sensors working at higher working temperature cause for ignition of fire related accidents and also consume more energy. They reveal sensing characteristic for multiple gases. Hence, it is necessary to fabricate sensors having high selectivity towards particular gas. The chlorine ($Cl_2$) is one of the poisonous gases that can cause health problems upon its inhalation. Moreover, also it is highly irritating, extremely reactive, destructive to living tissues and potentially lethal. Thereby, developing low-temperature $Cl_2$ gas sensors with good selectivity and fast response time is on priority. Till date, titanium dioxide ($TiO_2$) has not been much explored for gas sensors as there are a few reports available on $TiO_2$-based gas sensors even though it is non-toxic, abundantly available, cheap with excellent electrical and optical properties [12]. It is basically an *n*-type semiconducting wide-band gap material of promising applications not only in gas detection [13], solar cells, self-cleaning glasses, water purification, but also in food product industries as it shows potential biological activities like anti-fungal. This is because of the existence of three phases *viz.* rutile, anatase and brookite with different chemical, electrical, structural and optical properties. Further, the gas sensing properties can be improved in terms of fast response, low-operating temperature and good selectivity by decorating noble metal NPs on metal oxide sensor surface [14-22]. Several methods have been established for $TiO_2$ synthesis such as chemical bath deposition [12], sol-gel [23], hydrothermal [24] and so on. Researchers also are attracting to develop biological methods [25-27], which are basically eco-friendly and have several advantages over chemical methods low synthesis temperature, cost-effective and free from chemical reactions that eventually produce hazardous waste as by-products.

Present work is novel in terms of both i.e. synthesis of $TiO_2$ NPs and $Cl_2$ gas sensor application. Efforts have been made to study the selectivity and gas sensing properties of $TiO_2$ NPs. For this purpose, in the present work, bio-synthesized $TiO_2$ NPs were envisaged for gas sensing application. The $TiO_2$ NPs were characterized by using standard material characterization tools. The gas sensing properties of $TiO_2$ NPs were investigated for various gases where $Cl_2$ has revealed an optimum performance thereby, the $Cl_2$ sensing properties were performed as function of operating temperature and gas concentration with error limit. The transient responses for both sensors were also studied for knowing respective response and recovery time values. The repeatability and stability tests of both sensor materials were recorded and reported.

## METHODOLOGY

The biosynthesis method used for the synthesis $TiO_2$ nanoparticles (NPs) was adopted from our previous report Ekar et al. [27]. In a typical biosynthesis process, the extract of *Ganoderma* mushroom was prepared by boiling *Ganoderma* mushroom fine powder in 100 ml double distilled water at 85 °C for 15 min. The extract was filtered and stored as a stock solution at 4 °C. The 0.15 M titanium (Ti) precursor solution in ethyl alcohol was prepared by using titanium tetraisopropoxide. The 5 ml of extract was drop-wise added into 50 ml of 0.5 M Ti-precursor solution. The as-prepared precipitate was dried and annealed at 450 ˚C for 2 h to obtain $TiO_2$ powder. The glass pieces of 2 cm x 6 cm dimensions were used as substrates for preparation of sensor film of as-annealed $TiO_2$ powder by using doctor-blade method. The glass substrates were cleaned by using soap solution followed by ultrasonication in deionized water and ethanol. For making sensor film on pre-cleaned glass substrate, 0.1 gm/ml concentration of

$TiO_2$ powder in deionized water was used in the presence of polyvinyl alcohol binder. The resultant as-prepared film was air-annealed at 200 °C for 2 h in order to remove binder. The $TiO_2$ NPs film was employed for materials characterizations and gas sensing properties measurements by various means. The materials characterization of films was done by using X-ray diffraction, field emission scanning electron microscopy and UV-Visible spectroscopy. To study the gas sensing characteristics, two silver contacts at 10 mm apart from each other were given on the top surface of $TiO_2$ NPs sensor film by using commercial silver paste.

The sensor film was mounted onto a heating plate in a sealed chamber and measured stabilized resistances ($R_a$) in the air and ($R_g$) in the presence of target gas. The gas response was obtained by using the relation (1).

$$S\ (\%) = \frac{|R_a - R_g|}{R_a} * 100 \quad (1)$$

The gas sensing properties of $TiO_2$ NPs films were obtained by using a computer interfaced home-built static gas sensing system.

## RESULTS AND DISCUSSION

The X-ray diffraction (XRD) pattern of pure $TiO_2$ NPs film is shown in figure -1. The presence of diffraction peaks in XRD pattern confirm the pyramidal crystal structure with anatase phase (JCPDS card no. 21-1272) [5, 24, 27] in resultant film. The occurrence of sharp

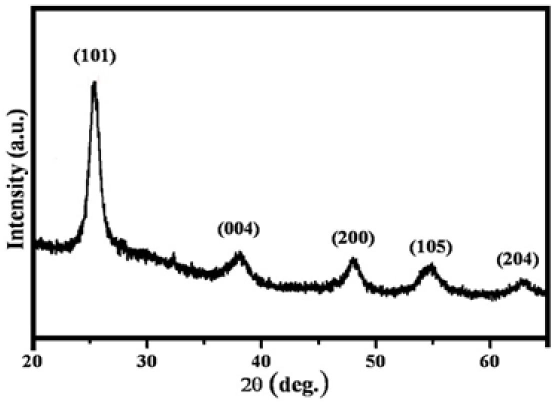


**Figure 1**. The X-ray diffraction (XRD) pattern of pure $TiO_2$ NPs film

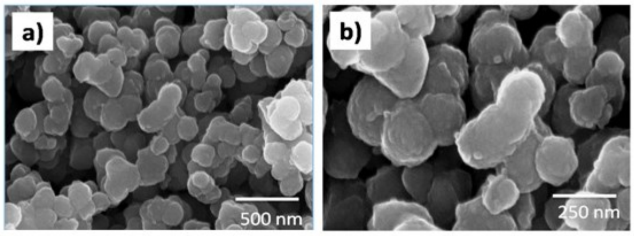


**Figure2**. Field emission scanning electron micrographs (FESEM ) of $TiO_2$ NPs films at two different magnifications.

diffraction peaks indicates good crystallization and involvement of no impurity peaks. It reported that the gas sensing properties of sensors based on metal oxides are influenced by structural parameters such as crystallite-size, texture coefficient (TC), dislocation densities [28 - 31] etc. The average value of crystallite size obtained from all diffraction peaks by using Scherer's relation is found to be of 7.2 nm. The maximum TC value of 1.22 is associated with (101) plane, which indicates the preferred growth direction of as-prepared $TiO_2$.

The field emission scanning electron micrographs (FESEM) of $TiO_2$ NPs films at two different magnifications were carried out and are shown in figure - 2 (a-b). The nanoparticles (NPs)-like morphology of $TiO_2$ is confirmed from FESEM images. The energy dispersive spectrum (EDS) of $TiO_2$ NPs film surface showed the presence of peaks corresponding to only Ti and O. This confirms the purity of result films. The optical properties of $TiO_2$ NPs film was investigated by using UV-Visible spectroscopy. The UV-visible spectrum of $TiO_2$ NPs film is shown in figure -3. The UV absorbance peak was observed in ultra-violet region. The optical band gap value of $TiO_2$ NPs film was estimated from Tauc plot. The Tauc's relation of photon energy ($h\upsilon$) with absorption coefficient ($\alpha$) is given as [3] in relation (2).

$$\alpha = \frac{\alpha_o\ (h\upsilon - E_g)^n}{h\upsilon} \quad (2)$$

where, $E_g$ = band gap energy, $\alpha$ = absorption coefficient, $\alpha_O$ = constant.

The value of 'n' depends on the type of transition. The 'n' has values 1/2. The Tauc plot is shown as a inset of figure - 3. The optical energy band gap energy of $TiO_2$ NPs film is calculated to be 3.3 eV.

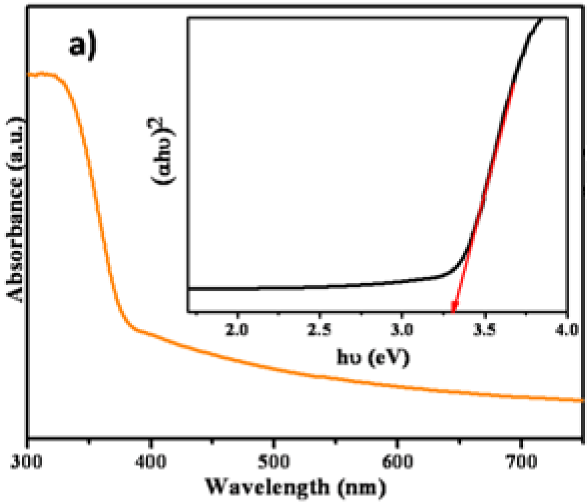


**Figure 3**. UV-visible spectrum of $TiO_2$ NPs film (inset: Tauc plot- variation of $(\alpha h\upsilon)^2$ versus photon energy, hυ (eV))

The $TiO_2$ NPs films were investigated for gas sensing properties. Generally, metal oxide gas sensors work at higher operating temperatures i.e. ≥ 150 °C. The adsorption/desorption of target gas molecules get affected due to increasing operating temperature. Optimization of operating temperature of present sensor is essential.

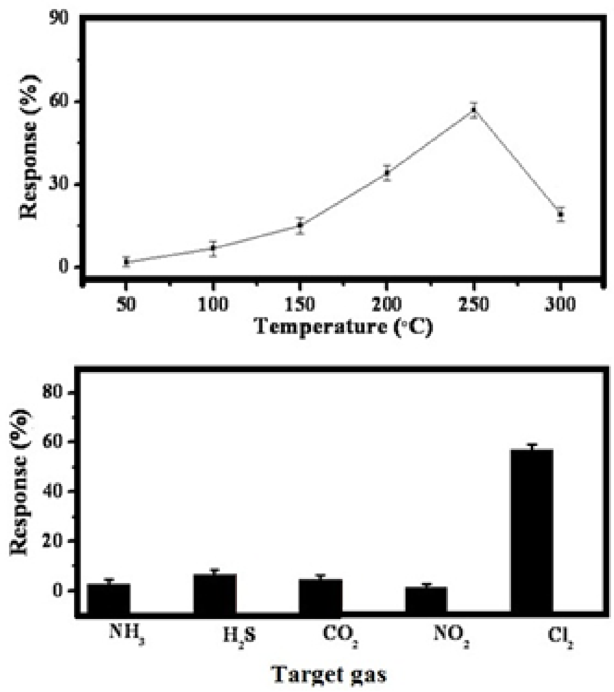


**Figure 4**. The variation of sensor response at different operating temperatures for $TiO_2$ NPs film at 100 ppm of $Cl_2$ target gas (Top) and sensor response for $TiO_2$ NPs film at 100 ppm for different test gases.

The sensors were studied for $Cl_2$ (keeping 100 ppm) at various operating temperatures (figure – 4 top). It was observed that the $TiO_2$ NPs film reveals highest $Cl_2$ response of 57 % at 250 °C operating temperature. Involvement of oxygen vacancies, which act as defects, is responsible for an *n*-type semiconducting behaviour of $TiO_2$. Hence, electrons are the majority charge carriers in conduction band. The basis for sensor working is the change of its resistance on the exposure of the target gas. The resistance of $TiO_2$ NPs sensor film is increased after $Cl_2$ gas exposure. A typical $Cl_2$ gas sensing mechanism has been explained for '*n*' type metal oxide semiconductor gas sensor by Navale et al. [32].

These sensors are further employed to check their responses for various gases besides $Cl_2$ such as $NH_3$, $H_2S$, $CO_2$, $NO_2$. The figure – 4 (bottom) gives the sensor response for $TiO_2$ NPs film at 100 ppm for different test gases: $NH_3$, $H_2S$, $CO_2$, $NO_2$ and $Cl_2$. It is observed that present sensors have good selectivity towards $Cl_2$ gas. The transient $Cl_2$ gas responses for $TiO_2$ NPs film sensors are also studied. As the $Cl_2$ gas injected in testing system, the target gas molecules diffuse through air and gets adsorbed onto the sensor surface for catalytic sensing reaction with time. As the time progresses, this sensor shows response in increasing order till saturation or equilibrium level for given concentration of target gas is achieved. At saturation level, sensor shows constant response. After gas testing system opened to an external atmosphere, the target gas molecules start desorbing and corresponding sensor response also decreases. The time taken by sensor to reach 90% of change in response or resistance value for given concentration of target gas is nothing but the response time. Similarly, recovery time can be also recorded. The response time value for $TiO_2$ NPs film sensor is recorded to be 97 s. The recovery time value for $TiO_2$ NPs film sensor is found to be 56 s.

The repeatability and transient gas response studies for $TiO_2$ NPs films are also studied. The good repeataiblities are observed for $TiO_2$ NPs film sensor at 100 ppm concentration of $Cl_2$ target gas.

The $Cl_2$ concentration effect on the gas response and stability for $TiO_2$ NPs film sensor was performed. The figure – 5 (top) gives the variation of $TiO_2$ NPs film sensor response at different concentration (ppm) of $Cl_2$ target gas. The $Cl_2$ gas concentration was varied from 5 to 400 ppm for both the sensors. It is observed that both the sensors show lower gas response for less concentration of $Cl_2$ gas. As concentration of $Cl_2$ increases the corresponding responses are also increased.

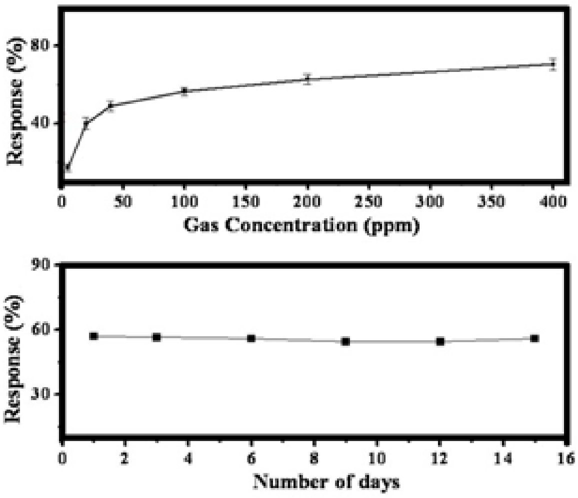


**Figure 5**. Variation of $TiO_2$ NPs film sensor response at different concentration (ppm) of $Cl_2$ target gas (top) and variation of $TiO_2$ NPs film sensor response at 100 ppm of $Cl_2$ target gas at different time intervals (bottom)

The response to maximum $Cl_2$ gas concentration is restricted by available area of sensor surface. As sensor surface area is limited, the sensor gets saturated meaning shows constant response for higher gas concentration.The stability of sensors was confirmed after periodic time interval. The figure – 5 (bottom) gives the variation $TiO_2$ NPs film sensor response for 100 ppm concentration of $Cl_2$ target gas at different time interval. It is observed that sensor shows good stability. All gas sensing studies were performed several times with good repeatability and stability with standard.

## CONCLUSION

In summary, bio-synthesized $TiO_2$ NPs film sensors are characterized for their structures and morphologies and investigated for gas sensing properties. The sensors show good selectivity towards $Cl_2$ gas sensing. The $TiO_2$ sensor shows highest $Cl_2$ gas response of 57 % for 100 ppm at 250 °C operating temperature. The response and recovery times for $TiO_2$ NPs film sensor are found to be 97 s and 56 s respectively. The lower $Cl_2$ detection is observed at 5 ppm concentration whereas, for higher concentration at 400 ppm. The present sensors highlight good repeatability and stability for $Cl_2$ sensing. Bio-synthesis of $TiO_2$ is economical method and is an easy way for developing commercial gas sensors.

**Conflicts of interest:** The authors stated that no conflicts of interest.

## REFERENCES


1. Nakate UT, Patil P, Bulakhe RN, Lokhande CD, Kale SN, Naushad M, and Mane RS. Sprayed zinc oxide films: Ultra-violet light-induced reversible surface wettability and platinum-sensitization-assisted improved liquefied petroleum gas response, *J. Coll. Interfaces Sci.*, 2016; 480: 109-117.
2. Mirzaei H, and Darroudi M. Zinc oxide nanoparticles: Biological synthesis and biomedical applications, *Ceram. Inter.*, 2017; 43(1): 907-914.
3. Zhang J, Shao Y, Hsieh CT, Chen YF, Su TC, Hsu JP, and Juang RS. Synthesis of magnetic iron oxide nanoparticles onto fluorinated carbon fabrics for contaminant removal and oil-water separation, *Separ. Purif. Tech.*, 2017; 174: 312-319.
4. Dhamodharan P, Manoharan C, Bououdina M, Venkadachalapathy R, and Ramalingam S. Al-doped ZnO thin films grown onto ITO substrates as photoanode in dye sensitized solar cell, *Solar Ener.*, 2017; 141: 127-144.
5. Krško O, Plecenik T, Roch T, Grančič B, Satrapinskyy L, Truchlý M, Ďurina P, Gregor M, Kúš P, and Plecenik A. Flexible highly sensitive hydrogen gas sensor based on a $TiO_2$ thin film on polyimide foil, *Sens. Actuators B: Chem.*, 2017; 240: 1058-1065.
6. Mishra RK, Upadhyay SB, Kushwaha A, Kim TH, Murali G, Verma R, Srivastava M, Singh J, Sahayb PP, and Lee SH. $SnO_2$ quantum dots decorated on RGO: a superior sensitive, selective and reproducible performance for a $H_2$ and LPG sensor, *Nanoscale*, 2015; 7(28): 11971-11979.
7. Zhang Y, Liu C, Gong F, Jiu B, and Li F. Large scale synthesis of hexagonal simonkolleit nanosheets for ZnO gas sensors with enhanced performances, *Mater. Lett.*, 2017; 186: 7-11.
8. Liu Y, Huang J, Yang J, and Wang S. Pt nanoparticles functionalized 3D $SnO_2$ nanoflowers for gas sensor

application, *Solid-State Electronics*, 2017; 130: 20-27.

9. Shendage SS, Patil VL, Vanalakar SA, Patil SP, Harale NS, Bhosale JL, Kim JH, and Patil PS. Sensitive and selective $NO_2$ gas sensor based on $WO_3$ nanoplates, *Sens. Actuators B: Chem.*, 2017; 240: 426-433.
10. Cindemir U, Trawka M, Smulko J, Granqvist CG, Österlund L, and Niklasson GA, Fluctuation-enhanced and conductometric gas sensing with nanocrystalline NiO thin films: A comparison, *Sens. Actuators B: Chem.*, 2017; 242: 132-139.
11. Wang Y, Liu J, Wang M, Pei C, Liu B, Yuan Y, Liu S, and Yang H. Enhancing the sensing properties of $TiO_2$ nanosheets with exposed {001} facets by a hydrogenation and sensing mechanism, *Inorg. Chem.*, 2017; 56 (3): 1504–1510.
12. Singh AK, Patil SB, Nakate UT, and Gurav KV. Effect of Pd and Au sensitization of bath deposited flowerlike $TiO_2$ thin films on CO sensing and photocatalytic properties, *J. Chem.*, 2013; Article ID 370578.
13. Eranna G. Metal oxide nanostructures as gas sensing devices; CRC Press: Boca Raton, FL, U.S.A., 2012.
14. Nakate UT, Bulakhe RN, Lokhande CD, and Kale SN. Au sensitized ZnO nanorods for enhanced liquefied petroleum gas sensing properties, *Appl. Surf. Sci.*, 2016; 371: 224–230.
15. Zou AL, Qiu Y, Yu JJ, Yin B, Cao GY, Zhang HQ, and Hu LZ. Ethanol sensing with Au-modified ZnO microwires, *Sens. Actuators B: Chem.*, 2016; 227: 65–72.
16. Kaneti YV, Yue J, Moriceau J, Chen C, Liu M, Yuan Y, Jiang X, and Yu A. Experimental and theoretical studies on noble metal decorated tin oxide flower-like nanorods with high ethanol sensing performance, *Sens. Actuators B: Chem.*, 2016; 219: 83–93.
17. Samerjai T, Liewhiran C, Wisitsoraat A, Tuantranont A, Khanta C, and Phanichphant S. Highly selective hydrogen sensing of Pt-loaded $WO_3$ synthesized by hydrothermal/impregnation methods, *Int. J. Hydrogen Energy*, 2014; 39: 6120–6128.
18. Tong PV, Hoa ND, Duy NV, Le DTT, and Hieu NV. Enhancement of gas-sensing characteristics of hydrothermally synthesized $WO_3$ nanorods by surface decoration with Pd nanoparticles, *Sens. Actuators B: Chem.*, 2016; 223: 453–460.
19. Samerjai T, Tamaekong N, Liewhiran C, Wisitsoraat A, and Phanichphant S. $NO_2$ gas sensing of flame-made Pt-loaded $WO_3$ thick films, *J. Solid State Chem.*, 2014; 214: 47–52.
20. Şennik E, Onur Alev, and Öztürk ZZ. The effect of Pd on the $H_2$ and CO sensing properties of $TiO_2$ nanorods, *Sens. Actuators B: Chem.*, 2016; 229: 692-700.
21. Trunga DD, Hoaa ND, Tonga PV, Duya NV, Daob TD, Chungb HV, Nagaob T, and Nguyen Van Hieu, Effective decoration of Pd nanoparticles on the surface of $SnO_2$ nanowires for enhancement of CO gas-sensing performance, *J. Hazard. Mater.*, 2014; 265: 124–132.
22. Salunkhe RR, Dhawale DS, Patil UM, and Lokhande CD. Improved response of CdO nanorods towards liquefied petroleum gas (LPG): effect of Pd sensitization, *Sens. Actuators B: Chem.*, 2009; 136: 39–44.
23. Yin Q, Wang X, Zhang K, Guo X, and Shen G. Fabrication of mesoporous $TiO_2$ with high crystallinity by a fast sol–gel method, *J. Porous Mater.*, 2017; 24(1): 157-163.
24. Huang X, Meng L, Du M, and Li Y. $TiO_2$ nanorods: hydrothermal fabrication and photocatalytic activities, *J. Mater. Sci. Mater. Elect.*, 2016; 27(7): 7222 - 7226.
25. Jayaseelan C, Rahuman AA, Roopan SM, Kirthi AV, Venkatesan J, Kim SK, Iyappan M, and Siva C. Biological approach to synthesize $TiO_2$ nanoparticles using Aeromonas hydrophila and its antibacterial activity, *Spectrochimica Acta Part A: Molecular and Biomolecular Spectroscopy*, 2013; 107: 82-89.
26. Tarafdar A, Raliya R, Wang WN, Biswas P, and Tarafdar JC. Green synthesis of $TiO_2$ nanoparticle using Aspergillus tubingensis, *Adv. Sci., Engg. & Medicine*, 2013; 5 (9): 943-949.
27. Ekar SU, Shekhar G, Khollam YB, Wani PN, Jadkar SR, Naushad M, Chaskar MG, Jadhav SS, Fadel A, Jadhav VV, Shendkar JH, and Mane RS. Green synthesis and dye-sensitized solar cell application of rutile and anatase $TiO_2$ nanorods, *J. Solid State Electrochem.* DOI 10.1007/s10008-016-3376-3.
28. Xu C, Tamaki J, Miura N, and Yamazoe N. Grain size effects on gas sensitivity of porous $SnO_2$-based elements, *Sens. Actuators B: Chem.*, 1991; 3(2): 147-155.
29. Kumar M, Kumar A, and Abhyankar AC. Influence of texture coefficient on surface morphology and sensing properties of W-doped nanocrystalline tin oxide thin films, *Appl. Mater. Interfaces*, 2015; 7(6): 3571–3580.
30. Singh I, and Bedi RK. Studies and correlation among the structural, electrical and gas response properties of aerosol spray deposited self assembled nanocrystalline CuO, *Appl. Sur. Sci.*, 2011; 257: 7592–7599.
31. Jime´nez I, Arbiol J, Dezanneau G, Cornet A, and Morante JR. Crystalline structure, defects and gas sensor response to $NO_2$ and $H_2S$ of tungsten trioxide nanopowders, *Sens. Actuators B: Chem.*, 2003; 93: 475–485.
32. Navale ST, Jadhav VV, Tehare KK, Sagara RUR, Biswasa CS, Galluzzi M, Liang W, Patil VB, Mane RS, and Stadler FJ. Solid-state synthesis strategy of ZnO nanoparticles for the rapid detection of hazardous $Cl_2$, *Sens. Actuators B: Chem.*, 2017; 238: 1102–1110.